The American Journal of Pathology, Vol. 184, No. 3, March 2014

ELSEVIER

The American Journal of
PATHOLOGY
ajp.amjpathol.org

METABOLIC, ENDOCRINE, AND GENITOURINARY PATHOBIOLOGY

The Senescence-Associated Secretory Phenotype Promotes Benign Prostatic Hyperplasia

Paz Vital, Patricia Castro, Susan Tsang, and Michael Ittmann

From the Department of Pathology and Immunology, Baylor College of Medicine, and the Michael E. DeBakey Department of Veterans Affairs Medical Center, Houston, Texas

Accepted for publication November 4, 2013.

Address correspondence to Michael Ittmann, M.D., Ph.D., Department of Pathology and Immunology, Baylor College of Medicine, One Baylor Plaza, Houston, TX 77030. E-mail: mittmann@bcm.tmc.edu.

Benign prostatic hyperplasia (BPH) is characterized by increased tissue mass in the transition zone of the prostate, which leads to obstruction of urine outflow and considerable morbidity in a majority of older men. Senescent cells accumulate in human tissues, including the prostate, with increasing age. Expression of proinflammatory cytokines is increased in these senescent cells, a manifestation of the senescence-associated secretory phenotype. Multiplex analysis revealed that multiple cytokines are increased in BPH, including GM-CSF, IL-1α, and IL-4, and that these are also increased in senescent prostatic epithelial cells *in vitro*. Tissue levels of these cytokines were correlated with a marker of senescence (cathepsin D), which was also strongly correlated with prostate weight. IHC analysis revealed the multifocal epithelial expression of cathepsin D and coexpression with IL-1α in BPH tissues. In tissue recombination studies in nude mice with immortalized prostatic epithelial cells expressing IL-1α and prostatic stromal cells, both epithelial and stromal cells exhibited increased growth. Expression of IL-1α in prostatic epithelial cells in a transgenic mouse model resulted in increased prostate size and bladder obstruction. In summary, both correlative and functional evidence support the hypothesis that the senescence-associated secretory phenotype can promote the development of BPH, which is the single most common age-related pathology in older men. *(Am J Pathol 2014, 184: 721–731; http://dx.doi.org/10.1016/j.ajpath.2013.11.015)*

Benign prostatic hyperplasia (BPH) is an extremely common disease of older men. By the eighth decade of life, approximately 80% of men have anatomical evidence of BPH, and half of these men exhibit symptoms of this disease.[1] This benign growth of the prostate leads to obstruction of urine outflow and causes considerable morbidity in older men. Complications of BPH, such as acute urinary retention and urinary tract infection, can occasionally lead to death. Up to 30% of men may require treatment for this condition at some time in their lives, and in the United States more than one billion dollars is spent annually on the medical and surgical treatment of this disease.[2] Thus, BPH is a disease that affects the majority of older men and is of considerable medical importance, but its pathogenesis is still obscure.

There are three major zones in the prostate: peripheral, central, and transition. These are not simply anatomical or histological regions, but have different behaviors in the aging prostate. The transition zone (TZ), which is located around the prostatic urethra, gives rise to BPH. Although other factors can play a role in the symptom complex characteristic of BPH, the overgrowth of TZ tissue around the prostatic urethra is clearly of importance in the pathogenesis of this disease. The TZ commonly increases more than 30-fold in size during development of BPH, and both epithelial and stromal elements contribute to this growth.[3]

Cellular senescence is a process that limits proliferation of human cells (and animal cells in general).[4] The senescence response can be induced by a variety of cellular alterations.[5] Intrinsic senescence occurs in human cells in response to telomere shortening and/or telomere uncapping as a result of repeated rounds of cell division. Senescence

Supported by NIH grants R01-DK083244 (M.I.), P20-DK097775 (M.I.), T32-DK007763 (D.L.), T32-AG000183 (L.D.), and P30-CA125123 (Human Tissue Acquisition and Pathology, Genetically Engineered Mouse, and Proteomics cores) and by use of the facilities of the Michael E. DeBakey Veterans Affairs Medical Center.

P.V. and P.C. contributed equally to this work.

Disclosures: None declared.

http://dx.doi.org/10.1016/j.ajpath.2013.11.015

can also be induced by a variety of nontelomeric signals, such as oxidative stress, DNA damage, and inappropriate expression of oncogenes.[5,6] Cellular senescence is subject to complex regulation by p53, p16, and other key proteins.[5,6]

Senescent cells accumulate in human tissues,[7] including the prostate,[8,9] with increasing age. These senescent cells have altered function, including increased expression of proinflammatory cytokines, growth factors, and proteases—all of which may alter the function of adjacent cells.[10,11] This phenomenon is known as the senescence-associated secretory phenotype. The senescent cells that accumulate with increasing age may contribute to the aging phenotype and age-related pathologies by secreting factors that act in a paracrine manner on adjacent cells and extracellular matrix. Previous studies from our research group indicated that senescent prostatic epithelial cells express at least two proinflammatory cytokines, IL-1α and IL-8.[9,12–14] With the present study, we extend those initial studies and provide both correlative and functional evidence that the senescence-associated secretory phenotype can promote the development of BPH, which is the single most common age-related pathology of older men.

Materials and Methods

Tissue Acquisition

Samples of prostate from normal or hyperplastic TZ tissue were taken from radical prostatectomies; a small part of the tissue was cultured and the rest was snap-frozen in liquid nitrogen. The tissues were determined to be free of carcinoma, as described previously.[15] Paraffin-embedded tissues from radical prostatectomy specimens were used for tissue microarray (TMA) construction. All tissues were collected with informed consent with the approval of the Baylor College of Medicine Institutional Review Board.

Primary Epithelial Cell Culture

Prostatic TZ tissues were harvested and used to establish primary epithelial cultures; serial samples of cultures were collected for protein or RNA extraction. Primary prostatic epithelial cells were cultured in prostate epithelial growth medium with penicillin/streptomycin (Clonetics; Lonza, Walkersville, MD) and were passaged at approximately 80% confluence over a period of several weeks. Early-passage cells were highly proliferative; late-passage cells exhibited senescent morphology and were slow to replicate.

Tissue Culture

Human post-pubertal prostate PNT1a cells were obtained from the European Collection of Cell Cultures (Porton Down, UK) and maintained in RPMI 1640 medium with 10% fetal bovine serum (FBS). The human prostate stromal cell line 19I (described previously[16]) was obtained from Dr. David Rowley, Baylor College of Medicine. The 19I cells were cultured in FBS medium containing Dulbecco's modified Eagle's medium, 5% Nu-Serum (BD Biosciences, San Jose, CA), 5% FBS, 10 ng/mL insulin, 0.2 ng/mL testosterone, and penicillin–streptomycin antibiotics.

Transfection of PNT1a Cells with IL-1α cDNA

Human IL-1α was PCR amplified from a human cDNA pool using primers forward 5′-AAGTGAGATGGCCAAAGTTCC-3′ and reverse 5′-TCTTGGGCAGTCACATACAA-3′ and was cloned in-frame into pcDNA 3.1/V5-His TOPO (Life Technologies, Carlsbad, CA). Clones were screened by HindIII digestion to check orientation and PCR-amplified to verify the presence of the IL-1α insert. Positive clones were sequenced in two directions, to confirm sequence integrity. The vector was stably transfected into PNT1a cells using FuGENE 6 transfection reagent (Roche Diagnostics, Indianapolis, IN) according to the manufacturer's instructions, under Geneticin (Gibco; Life Technologies, Carlsbad, CA) selection. Control cells were established by transfecting an empty pcDNA 3.1/V5 vector. Protein expression was verified using an IL-1α enzyme-linked immunosorbent assay (ELISA) (R&D Systems, Minneapolis, MN).

Differential Reactive Stroma Model

We performed xenograft experiments using a variation of the differential reactive stroma model[17] to establish PNT1a tumors subcutaneously in nude mice. PNT1a control or PNT1a–IL-1α cells were combined with 19I stromal cells in a 4:1 ratio, with Matrigel, and were subcutaneously injected bilaterally in six mice for each group (2.5×10^6 total cells per injection). The cells were allowed to establish tumors and then were collected after 20 days and weighed. A portion of the tissue was fixed for histology, and a portion was frozen for molecular analysis.

Quantitative Assessment of SA-β gal Activity

Tissue lysates were used for quantitative senescence-associated β-galactosidase (SA-β-gal) assay as described previously.[9] In brief, lysates were prepared and 50 μg of total protein in 50 μL lysis buffer was placed in duplicate microtiter wells and 100 μL of SA-β-gal stain solution (pH 6.0) was added to each well. The plate was then incubated at 37°C for 20 hours and the optical density read at 590 nm. One unit of SA-β-gal activity was defined as the activity leading to 1 optical density unit at 590 nm in a 20 hour incubation.

ELISA

Tissue and cell extracts of protein prepared as described above were used for quantitative determination of p16 (E01A0001; BlueGene, Shanghai, China), cathepsin D (CTSD) (ab119586; Abcam, Cambridge, MA), or IL-1α (MLA00; R&D Systems) by ELISA based on a quantitative

sandwich immunoassay technique according to the manufacturer's instructions. Absorbance was measured at 450 nm using a VERSAmax tunable microplate reader (Molecular Devices, Sunnyvale, CA). All determinations were performed in triplicate.

Luminex xMAP Cytokine Analysis

The quantitative analyze of 41 human chemokine and cytokine analytes was performed using a MILLIPLEX MAP human cytokine/chemokine premixed 26-plex panel (Millipore, Billerica, MA). In brief, 40 different primary cell cultures were trypsinized and washed four times in PBS. Cells were spun down, snap-frozen in liquid nitrogen, and stored at −80°C until analysis. Primary cells and normal TZ ($n = 20$) or BPH ($n = 50$) prostate tissues were lysed using radioimmunoprecipitation assay buffer (Sigma-Aldrich, St. Louis, MO) with protease inhibitors. Lysates were cleared by centrifugation and then stored at −80°C. Protein lysates (10 μg) were analyzed for the presence of 40 different cytokines and chemokines. The analytes were as follows: EGF, eotaxin, FGF-2, Flt-3 ligand, fractalkine, G-CSF, GM-CSF, GRO, IFNα2, IFN-γ, IL-1ra, IL-1α, IL-1β, IL-2, sIL-2Rα, IL-3, IL-4, IL-5, IL-6, IL-7, IL-8, IL-9, IL-10, IL-12 (p40 and p70), IL-13, IL-15, IL-17A, IP-10, MCP-1, MCP-3, MDC, MIP-1α, MIP-1β, PDGF-AA, PDGF-AB/BB, RANTES, sCD40L, TGF-α, TNF-β, and VEGF. The plate was analyzed using a Bio-Plex 200 system, and data were analyzed using Bio-Plex manager software version 6.0 (Luminex, Austin, TX).

Western Blotting

Western blot analyses were performed as described previously,[18] using the primary antibody anti-CTSD (sc-53927; Santa Cruz Biotechnology, Santa Cruz, CA), with monoclonal anti−β-actin antibody (Sigma-Aldrich) as the protein loading control. Western blot signals were visualized using enhanced chemiluminescence (Thermo Fisher Scientific, Rockford, IL) and were exposed and developed with films or with a Bio-Rad imaging system and quantified using densitometer with Quantity One software version 4.5.2 (Bio-Rad Laboratories, Hercules, CA).

Tissue Microarrays

Samples of the prostate from the TZ were collected from paraffin-embedded blocks from men undergoing radical prostatectomy for localized prostate cancer. Patients were between the ages of 50 and 65 and received no adjuvant therapy such as radiation or hormonal therapy. All sample tissues were free of carcinoma. Formalin-fixed, paraffin-embedded tissues were used to construct a TMA using a manual tissue arrayer (Beecher Instruments, Silver Spring, MD; Estigen, Tartu, Estonia). The final TMA consisted of 7 cores of normal TZ tissues, 19 of BPH tissues, and 2 of control tissues. Each core was 2 mm in diameter; cores were arranged 0.2 mm apart vertically and horizontally. Array sections were cut at 5-μm thickness.

Immunohistochemistry

IHC analyses of the human prostate TMA, mouse prostate tissues, and xenograft tissue were conducted using formalin-fixed, paraffin-embedded sections. After deparaffinizing and rehydrating of the tissue section, antigen retrieval was performed for 20 minutes in a rice steamer in Tris−EDTA buffer, pH 8.0 (Sigma-Aldrich). For single IHC, primary antibodies anti-SV40 large T antigen (1:500; sc20800; Santa Cruz Biotechnology, Santa Cruz, CA), anti−IL-1α (1:200; SC-7929; Santa Cruz Biotechnology), anti-CD31 (1:40; CM303; Biocare Medical, Concord, CA), anti−Ki-67 (1:400; RM-9106; Thermo Fisher Scientific, Waltham, MA), or anti-CTSD (1:50; 2510-1; Abcam) were diluted in Renaissance antibody diluent (Biocare Medical). Sections were incubated with the primary antibody for 2 hours at room temperature and developed using the avidin−biotin peroxidase complex procedure (Vector Laboratories, Burlingame, CA). The detection of the antibody was performed for horseradish peroxidase visualization using 3,3′-diaminobenzidine (Stable DAB Plus; Diagnostic BioSystems, Pleasanton, CA) for 2 minutes at room temperature. For double IHC of the TMA, the same antibodies were used for IL-1α and CTSD at the same dilutions. The TMA section was first incubated with the IL-1α primary antibody overnight at 4°C. Detection was performed as described above. The anti-CTSD antibody was then incubated for 2 hours at room temperature; Red AP visualization was then performed using an alkaline phosphatase substrate kit no. 1 (Vector Laboratories) for 10 minutes at room temperature. Finally, the tissue section was counterstained in Mayer's hematoxylin, dehydrated, and stabilized with mounting medium.

Image Analysis

Images were captured using a Vectra automated multispectral imaging system (PerkinElmer, Waltham, MA). For the analysis of Ki-67, we used InForm image analysis software version 1.2 (PerkinElmer) to separately analyze epithelium and stroma to quantify the number of positive nuclei in these two cell types. For CD31, we quantified the number of positive cells. For SV40 T antigen, we used ImageJ software version 1.45s (NIH, Bethesda, MD) to enumerate positive staining nuclei and total nuclei. Colocalization analysis of CTSD and IL-1α was performed using Nuance software version 3.0 (PerkinElmer). This software is capable of separating out individual chromogens and generates images for each antigen; the images can then be overlapped to generate the colocalization image. For each analysis, we established the threshold conditions before the batch analysis was conducted.

Transgenic Construct Cloning

The mouse IL-1α cDNA was PCR amplified from I.M.A.G.E. Consortium clone 3599550 (GenBank accession

no. BC003727; *http://www.ncbi.nlm.nih.gov/genbank*) (Open BioSystems; Thermo Scientific, Pittsburgh, PA) and subcloned into pCR2.1-TOPO (Life Technologies). Forward and reverse primers were tagged with EcoRI consensus sequences. The forward primers were modified to improve the Kozak consensus sequence for transcription initiation (5′-GAATTCGCCACCATGGCCAAAGTTCCT-3′ and 5′-GAATTCATAGACTCCCGAAATAAG-3′). The plasmid insert was sequenced in both directions using T7 and M13 reverse primers to ensure that no mutations occurred during amplification. The IL-1α cDNA was excised with EcoRI and ligated into the multiple cloning site on the ARR_2PB-KBPA vector containing the ARR_2PB promoter, CKR intron, and bGHpA[19] (courtesy of Dr. David Spencer, Baylor College of Medicine). Colonies were screened by PCR amplification and sequenced to identify clones in the appropriate orientation and to verify sequence. EcoRI-digested, gel-purified plasmid DNA was used at the Baylor College of Medicine Mouse Genetically Engineered Mouse core facility for microinjection into FVB mouse egg pronuclei. All experiments and animal work involving transgenic mice and wild-type littermates were conducted according to the animal protocol approved by the Baylor College of Medicine Institutional Animal Care and Use Committee.

After microinjection, 25 pups were born from five litters. DNA was prepared from tail cuttings and screened for the presence of the transgene using primers forward (ARR_2PB): 5′-CTGGTCATCATCCTGCCTTT-3′ and reverse (IL-1α): 5′-TCAGAATCTTCCCGTTGCTT-3′. Twelve-week-old transgenic and WT littermates were sacrificed to detect levels of IL-1α gene expression in the prostates of F1 progeny by quantitative RT-PCR using SYBR Green quantitative PCR on an iQ thermal cycler (Bio-Rad Laboratories).[20] IL-1α was amplified using the primer pair forward 5′-CATCAGCTGCTTATCCAGAGC-3′ and reverse 5′-ACTCCCGAAATAAGGCTGCT-3′ from cDNA pools of 12-week-old transgenic mouse prostate tissues. A single transgenic line was developed from a founder that had high levels of IL-1α gene expression in prostate tissue.

After germline transmission of IL-1α was determined, prostates were harvested from transgenic mice and wild-type littermate controls between 3 and 18 months of age. All lobes of the prostate (ventral, dorsal, lateral, and anterior) were harvested *en bloc* and seminal vesicles and bladder were harvested separately. Prostates were weighed and portions were snap-frozen and/or fixed in neutral buffered formalin and paraffin-embedded for histology and IHC. In older mice, urine was collected from the bladder by inserting a needle directly into the bladder with a syringe and urine volume was measured before harvest of the prostate and seminal vesicles. Protein extracts were measured by IL-1α ELISA to confirm increased protein production in a subset of transgenic mouse prostates, relative to WT.

Results

CTSD Is a Marker of Cellular Senescence and Is Increased in BPH

We have previously shown that SA-β-gal, a marker of cellular senescence, is increased with increasing passage number of primary prostatic epithelial cells and is also significantly increased in epithelial cells in BPH tissues.[9] SA-β-gal is a histochemical marker that requires fresh tissue for enzymatic activity, limiting its usefulness for paraffin-embedded tissues. To validate new senescence markers, we performed primary cultures of prostatic epithelial cells from TZ tissues. Cells were collected at early passages, while actively proliferating, or were carried for multiple passages until senescent. The late-passage cells exhibited a senescent morphology; quantitative assay of SA-β-gal on protein extracts, using an assay developed previously by our research group,[9] indicated a significant increase in SA-β-gal activity in later passage cultures (Figure 1A). The classic senescence marker p16 was also significantly increased (Figure 1B).

CTSD has been identified as a marker of cellular senescence.[21] We therefore evaluated the expression of CTSD by Western blotting of early- and late-passage prostate epithelial cells. CTSD was increased in late-passage cells (Figure 1C). To quantitatively evaluate CTSD expression, we performed a CTSD ELISA using protein extracts from early- and late-passage prostate epithelial cells. There was a significant increase in CTSD in the senescent epithelial cultures (Figure 1D). Thus, CTSD is a robust marker of prostate epithelial senescence.

We then evaluated the expression of CTSD in normal prostatic TZ tissue and in BPH tissue. CTSD was significantly increased in BPH tissue, compared with normal TZ tissue, according to ELISA (Figure 2A). Of note, p16, as measured by ELISA, was also significantly increased ($P = 0.013$, *t*-test; data not shown). There was a highly significant correlation of CTSD levels and prostate weight ($r^2 = 0.539$, $P < 0.001$, Pearson product moment) (Figure 2B). We then performed IHC using a TMA containing cores of normal TZ and BPH tissue. There was a marked increase in CTSD expression in the epithelium of BPH tissues, compared with normal TZ tissues (Figure 2, C and D). We note that, similar to our SA-β-gal findings,[9] there was very significant variability in staining, which tended to be focal within epithelial acini and variable between tissue cores. Some staining of cells within the stroma was also noted (Figure 2D). Some of these cells appear to be macrophages, whereas others had spindled morphology and may represent senescent fibroblasts. However, the number of CTSD-expressing stromal cells was much smaller than the number of senescent epithelial cells.

Cytokines Up-Regulated in BPH Are Increased in Senescent Epithelial Cells and Correlate with CTSD in BPH

To identify cytokines that play a role in the pathogenesis of BPH, we performed quantitative analysis of 40 cytokines in 20

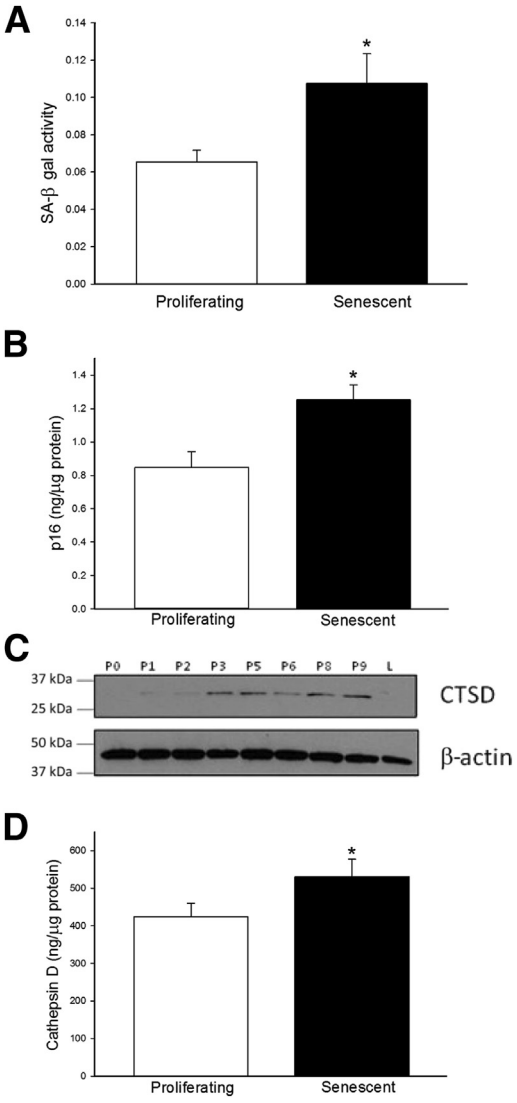

Figure 1 CTSD is a marker of prostatic epithelial senescence. **A:** SA-β-gal activity in extracts from proliferating and senescent epithelial cells, expressed in units, where 1 unit equals 1 OD at 590 nm in 20 hours. **B:** p16 protein levels in extracts from proliferating and senescent epithelial cells. **C:** Western blot of CTSD with protein lysates from primary prostatic epithelial cells at passages P0 to P9. Lane L, LAPC4 prostate cancer cell lysate. β-Actin is a loading control. **D:** CTSD protein levels as determined by ELISA in proliferating and senescent prostatic epithelial cells. Data are expressed as means ± SEM. $*P < 0.05$, *t*-test.

normal TZ tissues and 50 BPH tissues, using Luminex bead arrays. Numerous cytokines were increased in BPH tissue; however, because of significant variation in tissue levels, the increase was significant in only a subset of cytokines (Figure 3A). Both IL-1α and IL-8 were significantly increased in BPH, consistent with our previous observations.[12,14] We then analyzed the expression of the cytokines increased in BPH in protein extracts from early- and late-passage prostatic epithelial cells, using the same the Luminex technology. In all cases, the cytokines increased in BPH were also increased in the senescent epithelial cells (Figure 3B). Of note, IL-1α could not be quantitated, because in the senescent epithelial cells IL-1α was markedly increased and was higher than the linear range in this multiplex assay. We then evaluated the correlation between the levels of CTSD and cytokines in the normal TZ and BPH tissues. IL-1α, IL-4, GM-CSF and IL-10 were all highly correlated with CTSD levels (Table 1). Several other cytokines, including IL-8, IL-15 and IL-17, trended to correlation with CTSD but did not reach statistical significance. Taken together, the data indicated that the senescence-associated secretory phenotype contributes significantly to the expression of multiple cytokines within BPH tissue and that the extent of cellular senescence is correlated with total prostate weight.

To directly show that the senescent epithelial cells express IL-1α, we performed double immunostaining with antibodies to both CTSD and IL-1α using our TMA. The double-stained slides were scanned with spectral imaging, and Nuance software was used to unmix the chromogens and produce composite images of overlapping CTSD and IL-1α. Staining was predominantly epithelial, and almost all cells stained yellow, indicating coexpression of CTSD and IL-1α (Figure 3C). These were variably distributed within epithelial acini, with focal and sometimes multifocal staining. This pattern was seen in both normal TZ and BPH, although the pattern was far more extensive in BPH tissues (Figure 3C). Occasional cells with only CTSD or IL-1α staining were seen, but these were rare. In focal areas, we saw staining of stromal cells as well (Figure 3C), but this was far less common than in epithelial cells.

IL-1α Promotes Tissue Growth in a Tissue Recombination Model System

Multiple cytokines were increased in cellular senescence and in BPH tissues. Among the most up-regulated was IL-1α. We have previously shown that IL-1α is significantly up-regulated in BPH[12]; the present data confirm this up-regulation, and also indicate the correlation of IL-1α with epithelial senescence. We therefore sought to determine the functional significance of increased IL-1α in benign prostatic tissue growth. Rowley and colleagues[17] established the differential reactive stroma model, a model system for understanding the role of stroma in prostate cancer progression. In this model, LNCaP cancer cells are subcutaneously inoculated with human prostate stromal cell lines with or without Matrigel in nude mice. To use this model to study the role of paracrine interactions between nonneoplastic prostatic epithelial and stromal cells in BPH, we used PNT1a cells (a SV40 T antigen immortalized but nontumorigenic prostatic epithelial cell line established from normal epithelium[22]). We expressed IL-1α in PNT1a cells to mimic the epithelial expression of IL-1α in BPH epithelial cells. These cells (or vector controls) were then mixed with the human prostate stromal cell line 19I and growth factor–reduced Matrigel and inoculated subcutaneously in nude mice. After 20 days, tumors were collected and size was measured. Tumor size was significantly higher in IL-1α expressing tissues than in vector

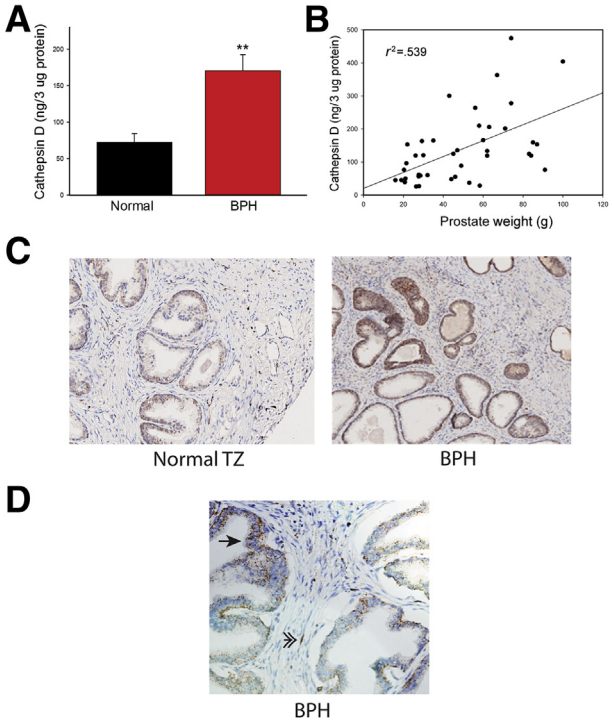

Figure 2 CTSD is increased in BPH and correlates with prostate weight. **A:** CTSD protein levels as determined by ELISA in protein extracts from BPH and normal TZ tissues. **B:** Correlation of CTSD levels and prostate weight (r^2 = 0.539, $P < 0.001$, Pearson product moment). **C:** IHC for CTSD. Medium-power view of CTSD in normal TZ and BPH tissue. **D:** High-power view of BPH tissue, showing epithelial expression of CTSD (**arrow**) and expression in occasional spindle-shaped cells (**double arrow**). Data are expressed as means ± SEM. $^{**}P < 0.01$, *t*-test. Original magnification: ×100 (**C**); ×400 (**D**).

controls (Figure 4A). No tumors were seen with either stroma or epithelium inoculated separately (data not shown).

The tumors consisted of stromal cells with islands of epithelial cells with admixed Matrigel (Figure 4B). To confirm that the epithelial-appearing cells were indeed PNT1a cells, we performed IHC with anti-SV40 T antigen antibody. Approximately 40% of cells expressed SV40 T antigen (Figure 4B). Surrounding the SV40 T antigen–positive PNT1a cells were unstained cells with a predominantly spindle morphology, presumably representing 19I human stromal cells and/or mouse stromal cells, including endothelial cells. IHC with anti–IL-1α antibody confirmed expression of IL-1α in the PNT1a–IL-1α tumors (Figure 4B). Quantitative analysis of the number of SV40 T antigen–stained cells revealed an increase in total PNT1a cells per tumor in the tumors using PNT1a–IL-1α cells, compared with vector controls (Figure 4C). The number of non-SV40–expressing cells was also increased in the tumors of PNT1a–IL-1α cells: 466 ± 19 (means ± SEM), compared with 382 ± 22 for the vector control ($P = 0.01$, *t*-test). Thus, the increased size of the PNT1a–IL-1α tumors was due to both increased PNT1a cells and increased 19I-derived and/or mouse-derived stromal cells, indicative of paracrine crosstalk promoting growth and/or recruitment of such cells. Finally, because IL-1α can enhance angiogenesis,[23] we examined angiogenesis using anti-CD31 IHC and image analysis. The percentage of the tumor represented by endothelial cells was significantly higher in tumors from PNT1a IL-1α-expressing cells, compared with controls (Figure 4D). These findings show that, when expressed as an epithelial cytokine, IL-1α can promote tissue growth of both benign stroma and epithelium.

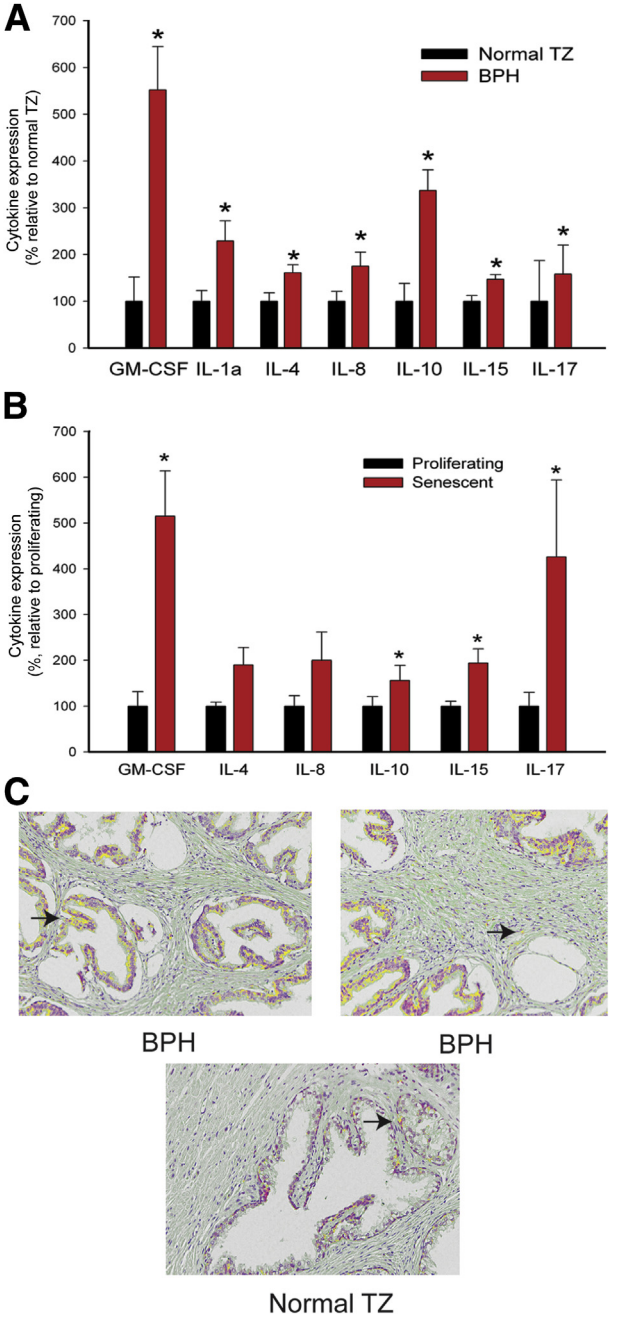

Figure 3 Increased expression of cytokines in BPH tissues and senescent prostatic epithelial cells. **A:** Expression levels of indicated cytokines as determined by Luminex assays in normal TZ and BPH tissues, relative to normal TZ (100%) for each cytokine. **B:** Expression level of the same cytokines (except IL-1α, which was out of the linear range in the assay in senescent cells) in extracts from proliferating and senescent epithelial cells, relative to proliferating cells (100%) for each cytokine. **C:** Double immunostaining with antibodies to CTSD (red) and IL-1α (green) of BPH and normal TZ tissues; yellow indicates coexpression (**arrows**). Staining was predominantly epithelial (**arrow**; BPH, **top left panel**). In focal areas, there was also some staining of stromal cells (**arrow**; BPH, **top right panel**). Data are expressed as means ± SEM. $^{*}P < 0.05$, *t*-test or *U*-test.

Table 1 Correlation of CTSD and Cytokine Levels in TZ Tissue Extracts

Cytokine	Correlation	*P* value
GM-CSF	0.44	<0.01
IL-1α	0.55	<0.001
IL-4	0.47	<0.01
IL-8	0.29	0.09
IL-10	0.46	<0.01
IL-15	0.252	0.142
IL-17	0.31	0.07

Prostate Epithelial Expression of IL-1α Results in Increased Prostate Size and Bladder Obstruction in a Transgenic Mouse Model

To evaluate the potential role of IL-1α in promoting prostatic growth, we constructed transgenic mice in which IL-1α is expressed under the control of the ARR_2PB prostate-specific promoter. This promoter directs prostate epithelial-specific expression of the transgene at the onset of sexual maturity in the transgenic male mice. Transgenic mice were analyzed for expression of IL-1α, and a mouse line with marked overexpression of IL-1α protein in the prostate after the onset of sexual maturity was established (ELISA; data not shown). These mice were monitored and analyzed for gross and microscopic prostatic pathology at intervals over the course of more than 18 months. A significant increase in total prostate weight was noted in mice over the age of 12 months (Figure 5A). This was accompanied by a marked increase in urine volume in these mice at the time of euthanasia, consistent with bladder outlet obstruction (Figure 5, B and C). IHC and image analysis for Ki-67, a proliferation marker, indicated a significant increase in proliferating epithelial and stromal cells in the prostate of the transgenic mice, compared with littermate controls (Figure 5D). Histological analysis indicated variable histology, with focally increased numbers of epithelial cells in the ventral and/or dorsolateral prostate (Figure 5E), accompanied in some cases by stromal thickening and fibrosis of the normally very thin fibromuscular stroma surrounding epithelial acini (Figure 5E).

Discussion

A major question confronting BPH research is the underlying pathogenesis of the disease. Multiple factors have been implicated in BPH, including cellular senescence,

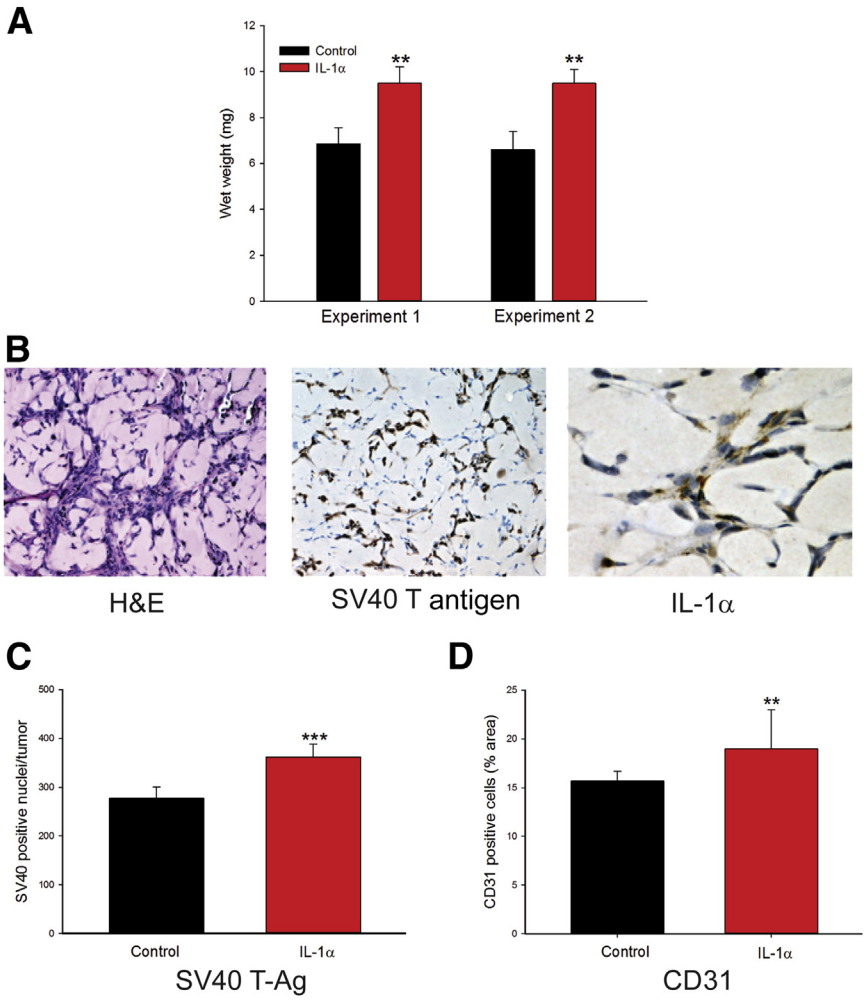

Figure 4 IL-1α enhances growth in a tissue recombination xenograft model. Immortalized but nontumorigenic prostatic epithelial cells (PNT1a) expressing IL-1α or vector controls were mixed with the prostate stromal cell line 19I and injected subcutaneously in nude mice. **A:** Tumor size at 20 days. **B:** PNT1a differential reactive stroma tumors stained with H&E show single cells and clusters of cells within a pale eosinophilic Matrigel (**left panel**). IHC for SV40 T antigen shows that approximately 40% of cells are PNT1a prostatic epithelial cells (**middle panel**). High-power view of PNT1a cells from PNT1a—IL-1α tumors showing cytoplasmic staining for IL-1α. No staining was seen in PNT1a tumors or in negative control sections (ie, without primary antibody) (**right panel**). **C:** Number of SV40 T angtigen positive nuclei per tumor section in control PNT1a and PNT1a—IL-1α tumors. **D:** Mean endothelial percentage assessed by anti-CD31 IHC and image analysis. Data are expressed as means ± SEM. $^{**}P < 0.01$, $^{***}P < 0.001$, *t*-test. Original magnification, ×100 (**B**, **left** and **middle panel**); ×400 (**B**, **right panel**).

alterations in hormones, and inflammation.[24,25] These factors may interact, and are not necessarily mutually exclusive players in the etiology of BPH.

Our present findings demonstrate, based on multiple markers, that senescent epithelial cells are significantly increased in BPH tissues, as are cytokines that are up-regulated as part of the senescence-associated secretory phenotype. Furthermore, the levels of multiple cytokines in BPH are strongly correlated with the degree of senescence in the tissue. Finally, functional studies indicated that, *in vivo*, at least one of the cytokines (IL-1α) can result in increased benign tissue growth in both xenograft and transgenic model systems. The growth-promoting activities of IL-1α may be due, in part, to induction of paracrine FGF-7 expression in adjacent stromal cells that can act on nonsenescent epithelial cells.[12] Jerde and Bushman[26] reported that IL-1α can also induce IGF-1 in prostatic stromal fibroblasts, further enhancing the epithelial growth response. Similarly, we reported that IL-8 can induce FGF-2 as a paracrine factor, which can stimulate both epithelial and stromal growth, and IL-8 can directly enhance growth of neighboring nonsenescent prosthetic epithelial cells.[13] Both FGF-2 and FGF-7 are significantly increased in BPH tissue.[27] Taken together, our findings strongly support the concept that cellular senescence of prostatic epithelial cells contributes significantly to the pathogenesis of BPH.

The presence of significant numbers of senescent epithelial cells in the prostate is in contrast to the findings in other organs, such as skin, where senescent stromal cells are more prominent.[7] This may reflect the low turnover rate of prostatic epithelium, as assessed by the relatively low number of proliferating cells,[28] in contrast to other epithelia (such as skin), which have a much higher turnover rate. This low mitotic activity in prostate tissue may make it less likely that there is significant erosion of telomeres within the prostatic epithelium because of replication. Thus, we believe that other mechanisms, such as oxidative stress and/or DNA damage, are inducing the senescence response in the prostatic epithelial cells. Olinski et al[29] reported that BPH tissues have higher levels of DNA base lesions typical of oxidative DNA damage in DNAs from BPH tissue (relative to matched normal tissue) and that in the majority of these patients there is a decreased activity of superoxide dismutase and/or catalase in the BPH tissues. Consistent with this finding, Malins et al,[30] using infrared spectroscopy, found higher levels of structural alterations in DNA from BPH tissue, consistent

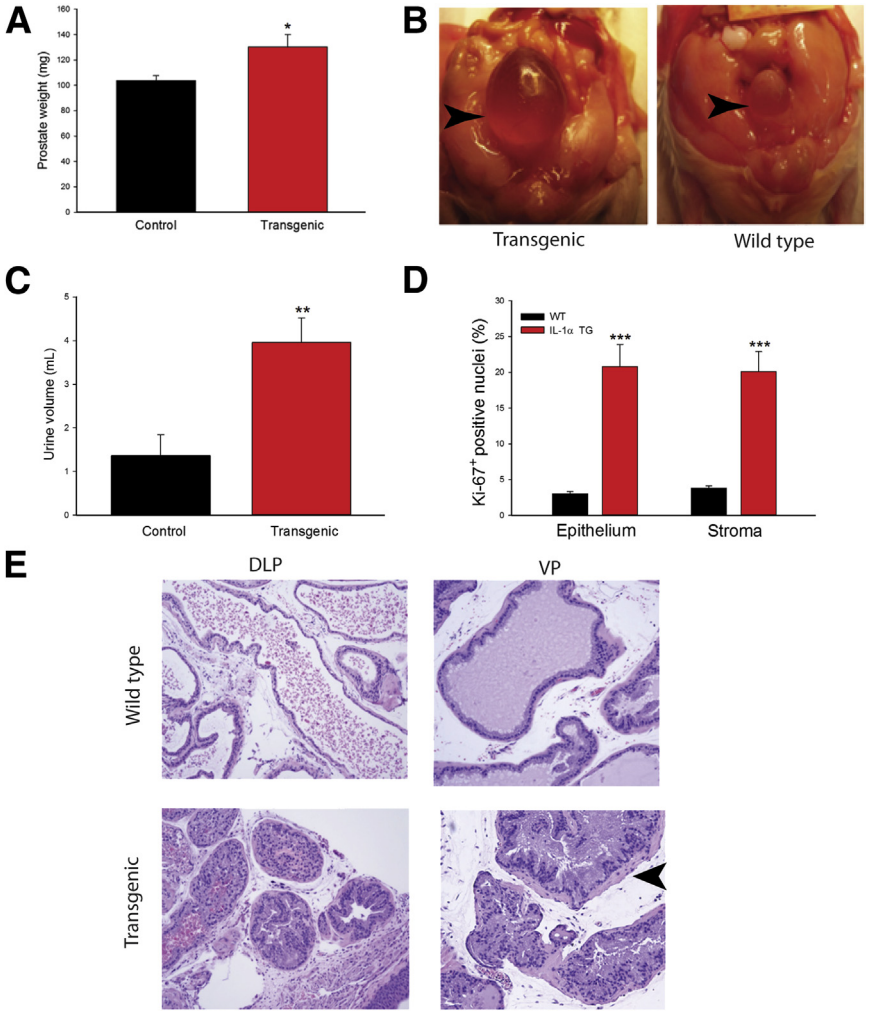

Figure 5 Phenotype of prostate-specific IL-1α transgenic mice. **A:** Mean prostate weight for ARR_2PB IL-1α transgenic mice and littermate controls. **B:** Example of enlarged bladder in ARR_2PB IL-1α transgenic mouse at time of euthanasia. **Arrowhead** indicates the bladder. **C:** Mean urine volume at time of euthanasia for ARR_2PB IL-1α transgenic mice and littermate controls. **D:** Mean percentage of Ki-67$^+$ nuclei in epithelium and stroma for ARR_2PB IL-1α transgenic mice and littermate controls. **E:** Histological appearance of dorsolateral and ventral prostates in ARR_2PB IL-1α transgenic mice and littermate controls. Thickening of the epithelium was seen, with areas of piling up. Stroma was focally thickened (**arrowhead**), compared with the fibromuscular stroma normally present in mouse prostate. Data are expressed as means ± SEM. $*P < 0.05$, $**P < 0.01$, and $***P < 0.001$, *t*-test. Original magnification, ×100. DLP, dorsolateral prostate; TG, transgenic; VP, ventral prostate.

with oxidative damage, compared with normal tissue. Expression microarray studies of aging rat prostate have revealed up-regulation of multiple genes that are increased during oxidative stress.[31] Superoxide dismutase gene expression was decreased in the prostate of older rats, a finding similar to protein expression data in human BPH.[31]

Barron and Rowley[32] reported induction of a reactive stroma phenotype in prostate cancer, and this reactive stroma was similar to the stroma seen in wound repair in a variety of sites. Schauer and Rowley[33] recently extended this concept to BPH. Cytokines from senescent epithelial cells can induce changes in prostatic stromal cells that are similar to the effects induced by the same cytokines (ie, IL-1α and IL-8) at wound sites, and senescence may act like a chronic wound biologically. A major feature of the reactive stroma is an increase in myofibroblasts. These cells, which are intermediate in phenotype between in fibroblasts and smooth muscle cells, are characteristic of reactive stroma. IL-8 can induce a myofibroblastic phenotype in prostatic fibroblastic *in vitro*, characterized by expression of smooth muscle α-actin (SMA) and tenascin, which are established markers of myofibroblasts.[16] Furthermore, IHC studies of IL-8 expression in BPH epithelium relative to normal TZ confirm the increased expression of IL-8 that we have observed in both the present and previous studies.[16] Importantly, quantitative studies have established that there is a significant increase in expression of the myofibroblast marker SMA in stromal cells adjacent to epithelial cells in BPH nodules, relative to normal TZ. These studies indicate that, in addition to inducing expression of growth factors and cytokines in stromal cells in a paracrine manner, there are changes in cellular differentiation into cells characteristic of reactive stroma that can be induced by cytokines secreted from senescent epithelial cells.

An important question is whether senescence of stromal cells also plays a role in the pathogenesis of BPH. We[9] and others[8] have not observed significant numbers of SA-β-gal–expressing prostatic stromal cells. This is in contrast to *in vitro* studies, in which prostatic stromal cells express SA-β-gal during senescence induced by a variety of conditions.[34] In other tissues, expression of SA-β-gal in stromal fibroblasts is a prominent feature in aging tissues. Recently, Bavik et al[34] reported that *in vitro* prostatic stromal fibroblasts express a variety of growth factors and cytokines when they undergo cellular senescence, including factors that we and others have found to be increased in BPH (including FGF-7, IL-8, and HGF).[12,13] It is possible that *in vivo* fibroblastic cells in the prostate do not accumulate SA-β-gal, although why this should be the case is unknown. We have, however, observed IL-8 in stromal cells in the prostate, although epithelial expression is more abundant.[13] Similarly, in the present study, we observed some stromal cells expressing CTSD. This is in agreement with the observations of Pruitt et al,[35] who observed small numbers of $CTSD^{+}$ stromal cells in benign prostate stroma (and focal staining in epithelial acini as well, based on their published IHC data). Interestingly, Pruitt et al[35] found increased CTSD in stromal cells in prostate cancer and showed that CTSD can promote cancer progression in tissue recombination models. Cherry et al[36] found that CTSD is present as an active form in prostate cancer, but in BPH it is present only in the inactive form. In BPH, CTSD is a marker of senescence and does not appear to play an active role in growth promotion. Thus, there appear to be significant differences in the biology of CTSD in stromal cells in cancer and in BPH. Overall, the data suggest that senescent stromal cells are present *in vivo* in BPH tissue, but are less abundant than senescent epithelial cells.

A major theory of BPH pathogenesis is that inflammation may promote the development of BPH. Quantitative studies have indicated that the vast majority of BPH tissues contain chronic inflammatory infiltrates, including both T and B

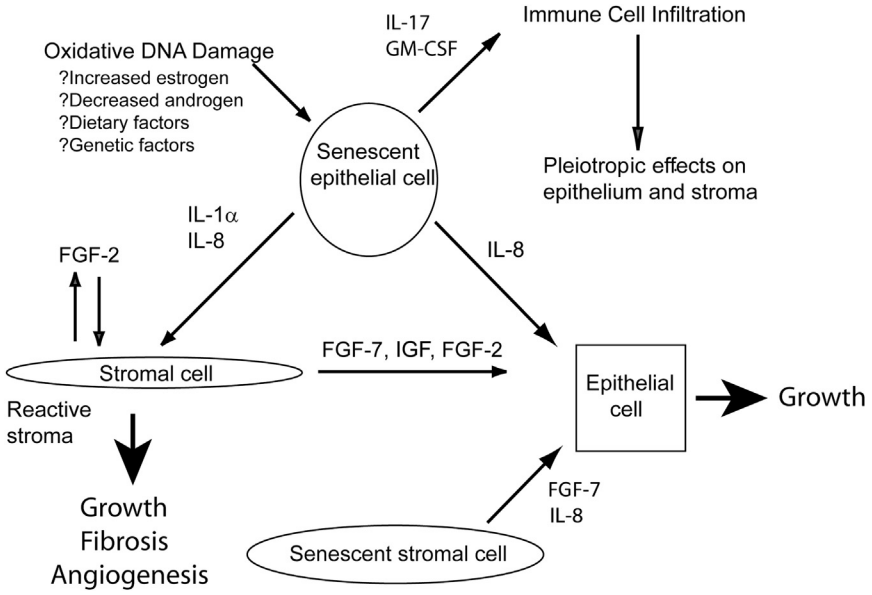

Figure 6 Model of BPH pathogenesis. Oxidative DNA damage results in epithelial senescence and initiation of the senescence-associated secretory response. Cytokines and growth factors released from senescent cells can directly promote growth of nonsenescent prostatic epithelium and stroma and can initiate paracrine loops, promoting growth of both cellular compartments. Secreted cytokines can also enhance influx of inflammatory cells into the prostate, which can lead to pleiotropic effects on prostate growth from factors secreted by these inflammatory cells. A reactive stroma phenotype is induced, which can promote fibrosis. Senescent stromal cells may also play a role, but are less common than senescent epithelial cells.

lymphocytes and macrophages. Kramer et al[37] reported that BPH tissues contain increased IL-4, and Steiner et al[38] reported increased IL-17 mRNA content in BPH tissues; both reports are consistent with our present results. IL-17 was expressed by infiltrating T lymphocytes, but also was noted focally in epithelial cell *in vivo*. IL-17 mRNA was detected in two of three BPH epithelial cell lines and in T cells isolated from BPH. IL-15, which can stimulate T lymphocyte recruitment, is expressed by prostatic stromal cells, and in BPH epithelial expression is also seen.[39] Our present data confirm that IL-4, IL-15, and IL-17 are all increased in BPH tissues. Furthermore, all of these cytokines are increased in senescent epithelial cells, and in BPH tissue there is a significant correlation between the content of IL-4 and the senescence marker CTSD. There is also a trend for correlation between tissue levels of CTSD and IL-15 and IL-17 in BPH tissue. Our present hypothesis is that senescence induces the expression of inflammatory cytokines that can act directly on adjacent tissues and also promote the influx of inflammatory cells into the prostate, which can then have extensive pleiotropic secondary effects leading to increased tissue growth, fibrosis, angiogenesis, and other pathological effects (Figure 6). Our hypothesis thus does not contradict the role of inflammation in BPH, but rather provides a potential explanation for the ubiquitous presence of inflammation within the aging prostate.

Our model for the pathogenesis of BPH is presented in Figure 6. We have placed cellular senescence at the center of this model, because expression of the senescence phenotype is correlated with expression of growth factors and cytokines that are, in turn, correlated with increasing net cellular proliferation in both the epithelial and stromal compartments, as well as with the severity of BPH *in vivo*. A major underlying cause of cellular senescence in the prostatic epithelial cells is oxidative DNA damage, although other causes of senescence may also contribute to this phenotype. Such oxidative DNA damage could be due, in part, to increased intraprostatic estrogens and decreased androgens, as well as to dietary and other environmental factors.

Our present findings support the concept that the TZ is more vulnerable to oxidative damage than the peripheral zone, because of lower levels of enzymes involved in protecting tissues from oxidative DNA damage. The senescent epithelial cells express proinflammatory cytokines (IL-8 and IL-1α, among others) that can have both direct and indirect effects leading to proliferation of adjacent nonsenescent epithelial and stromal cells. Our previous work demonstrated the importance of FGF-7 induction by IL-1α in the pathogenesis of BPH[12,27] and demonstrated that IGF-1 is also induced by IL-1α.[26] Similar studies have demonstrated both direct actions of IL-8 on epithelial proliferation and paracrine effects on stromal cells, leading to FGF-2 expression. Other paracrine and/or autocrine interactions are also a possibility. For example, expression of Kit ligand and HGF can be induced by IL-1α in nonprostatic fibroblasts.[40,41] The senescence-associated epithelial cytokines also alter the cellular phenotype of stromal cells in BPH tissue from a fibroblastic phenotype to a myofibroblastic phenotype characteristic of a reactive stroma. Such reactive stroma formation may result in collagen deposition and fibrosis. Recent studies have indicated that fibrosis of TZ tissues may play an important role in the symptom complex associated with benign BPH.[42–44] In addition, a number of cytokines released by senescent epithelial cells can attract inflammatory cells into the prostatic tissue, with further pathological effects contributing to the BPH phenotype. Growth factors and cytokines such as FGF-2, IL-1α, and IL-8 are also well known angiogenic factors and may promote angiogenesis, which is required to support the increased tissue present in the hyperplastic TZ. Senescent stromal cells may also contribute to the expression of growth factors and cytokines. Thus, our theory is that multiple factors that are directly or indirectly induced by epithelial senescence lead to the increased growth of epithelial and stromal tissues and fibrosis in BPH.

A central challenge in aging research is to determine whether senescent cells can lead to age-related pathologies and to define the pathophysiological mechanisms by which accumulation of senescent cells can lead to tissue dysfunction. The present work provides the beginning of a detailed mechanistic understanding of how cellular senescence can result in tissue alterations in the TZ of the prostate that lead to BPH, the most common age-related pathology in aging men.

Acknowledgment

We thank Billie Smith for technical assistance with IHC.

References

1. Glynn RJ, Campion EW, Bouchard GR, Silbert JE: The development of benign prostatic hyperplasia among volunteers in the Normative Aging Study. Am J Epidemiol 1985, 121:78–90
2. Wei JT, Calhoun E, Jacobsen SJ: Urologic Diseases in America project: benign prostatic hyperplasia. J Urol 2008, 179:S75–S80
3. Shapiro E, Hartanto V, Perlman EJ, Tang R, Wang B, Lepor H: Morphometric analysis of pediatric and nonhyperplastic prostate glands: evidence that BPH is not a unique stromal process. Prostate 1997, 33:177–182
4. Campisi J: Replicative senescence: an old lives' tale? Cell 1996, 84: 497–500
5. Ben-Porath I, Weinberg RA: The signals and pathways activating cellular senescence. Int J Biochem Cell Biol 2005, 37:961–976
6. López-Otín C, Blasco MA, Partridge L, Serrano M, Kroemer G: The hallmarks of aging. Cell 2013, 153:1194–1217
7. Dimri GP, Lee X, Basile G, Acosta M, Scott G, Roskelley C, Medrano EE, Linskens M, Rubelj I, Pereira-Smith O, Peacock M, Campisi J: A biomarker that identifies senescent human cells in culture and in aging skin in vivo. Proc Natl Acad Sci USA 1995, 92: 9363–9367
8. Choi J, Shendrik I, Peacocke M, Peehl D, Buttyan R, Ikeguchi EF, Katz AE, Benson MC: Expression of senescence-associated beta-

galactosidase in enlarged prostates from men with benign prostatic hyperplasia. Urology 2000, 56:160–166
9. Castro P, Giri D, Lamb D, Ittmann M: Cellular senescence in the pathogenesis of benign prostatic hyperplasia. Prostate 2003, 55:30–38
10. Coppé JP, Patil CK, Rodier F, Sun Y, Muñoz DP, Goldstein J, Nelson PS, Desprez PY, Campisi J: Senescence-associated secretory phenotypes reveal cell-nonautonomous functions of oncogenic RAS and the p53 tumor suppressor. PLoS Biol 2008, 6:2853–2868
11. Freund A, Orjalo AV, Desprez PY, Campisi J: Inflammatory networks during cellular senescence: causes and consequences. Trends Mol Med 2010, 16:238–246
12. Giri D, Ittmann M: Interleukin-1alpha is a paracrine inducer of FGF7, a key epithelial growth factor in benign prostatic hyperplasia. Am J Pathol 2000, 157:249–255
13. Giri D, Ittmann M: Interleukin-8 is a paracrine inducer of fibroblast growth factor 2, a stromal and epithelial growth factor in benign prostatic hyperplasia. Am J Pathol 2001, 159:139–147
14. Castro P, Xia C, Gomez L, Lamb DJ, Ittmann M: Interleukin-8 expression is increased in senescent prostatic epithelial cells and promotes the development of benign prostatic hyperplasia. Prostate 2004, 60:153–159
15. Wheeler TM, Lebovitz RM: Fresh tissue harvest for research from prostatectomy specimens. Prostate 1994, 25:274–279
16. Schauer IG, Ressler SJ, Tuxhorn JA, Dang TD, Rowley DR: Elevated epithelial expression of interleukin-8 correlates with myofibroblast reactive stroma in benign prostatic hyperplasia. Urology 2008, 72:205–213
17. Tuxhorn JA, McAlhany SJ, Dang TD, Ayala GE, Rowley DR: Stromal cells promote angiogenesis and growth of human prostate tumors in a differential reactive stroma (DRS) xenograft model. Cancer Res 2002, 62:3298–3307
18. Feng S, Dakhova O, Creighton CJ, Ittmann M: Endocrine fibroblast growth factor FGF19 promotes prostate cancer progression. Cancer Res 2013, 73:2551–2562
19. Seethammagari MR, Xie X, Greenberg NM, Spencer DM: EZC-prostate models offer high sensitivity and specificity for noninvasive imaging of prostate cancer progression and androgen receptor action. Cancer Res 2006, 66:6199–6209
20. Wang J, Yu W, Cai Y, Ren C, Ittmann MM: Altered fibroblast growth factor receptor 4 stability promotes prostate cancer progression. Neoplasia 2008, 10:847–856
21. Byun HO, Han NK, Lee HJ, Kim KB, Ko YG, Yoon G, Lee YS, Hong SI, Lee JS: Cathepsin D and eukaryotic translation elongation factor 1 as promising markers of cellular senescence. Cancer Res 2009, 69:4638–4647
22. Cussenot O, Berthon P, Berger R, Mowszowicz I, Faille A, Hojman F, Teillac P, Le Duc A, Calvo F: Immortalization of human adult normal prostatic epithelial cells by liposomes containing large T-SV40 gene. J Urol 1991, 146:881–886
23. Matsuo Y, Sawai H, Ochi N, Yasuda A, Takahashi H, Funahashi H, Takeyama H, Guha S: Interleukin-1alpha secreted by pancreatic cancer cells promotes angiogenesis and its therapeutic implications. J Surg Res 2009, 153:274–281
24. McLaren ID, Jerde TJ, Bushman W: Role of interleukins, IGF and stem cells in BPH. Differentiation 2011, 82:237–243
25. Lee KL, Peehl DM: Molecular and cellular pathogenesis of benign prostatic hyperplasia. J Urol 2004, 172:1784–1791
26. Jerde TJ, Bushman W: IL-1 induces IGF-dependent epithelial proliferation in prostate development and reactive hyperplasia. Sci Signal 2009, 2:ra49
27. Ropiquet F, Giri D, Lamb DJ, Ittmann M: FGF7 and FGF2 are increased in benign prostatic hyperplasia and are associated with increased proliferation. J Urol 1999, 162:595–599
28. Kyprianou N, Tu H, Jacobs SC: Apoptotic versus proliferative activities in human benign prostatic hyperplasia. Hum Pathol 1996, 27:668–675
29. Olinski R, Zastawny TH, Foksinski M, Barecki A, Dizdaroglu M: DNA base modifications and antioxidant enzyme activities in human benign prostatic hyperplasia. Free Radic Biol Med 1995, 18:807–813
30. Malins DC, Polissar NL, Gunselman SJ: Models of DNA structure achieve almost perfect discrimination between normal prostate, benign prostatic hyperplasia (BPH), and adenocarcinoma and have a high potential for predicting BPH and prostate cancer. Proc Natl Acad Sci USA 1997, 94:259–264
31. Reyes I, Reyes N, Iatropoulos M, Mittelman A, Geliebter J: Aging-associated changes in gene expression in the ACI rat prostate: implications for carcinogenesis. Prostate 2005, 63:169–186
32. Barron DA, Rowley DR: The reactive stroma microenvironment and prostate cancer progression. Endocr Relat Cancer 2012, 19:R187–R204
33. Schauer IG, Rowley DR: The functional role of reactive stroma in benign prostatic hyperplasia. Differentiation 2011, 82:200–210
34. Bavik C, Coleman I, Dean JP, Knudsen B, Plymate S, Nelson PS: The gene expression program of prostate fibroblast senescence modulates neoplastic epithelial cell proliferation through paracrine mechanisms. Cancer Res 2006, 66:794–802
35. Pruitt FL, He Y, Franco OE, Jiang M, Cates JM, Hayward SW: Cathepsin D acts as an essential mediator to promote malignancy of benign prostatic epithelium. Prostate 2013, 73:476–488
36. Cherry JP, Mordente JA, Chapman JR, Choudhury MS, Tazaki H, Mallouh C, Konno S: Analysis of cathepsin D forms and their clinical implications in human prostate cancer. J Urol 1998, 160:2223–2228
37. Kramer G, Steiner GE, Handisurya A, Stix U, Haitel A, Knerer B, Gessl A, Lee C, Marberger M: Increased expression of lymphocyte-derived cytokines in benign hyperplastic prostate tissue, identification of the producing cell types, and effect of differentially expressed cytokines on stromal cell proliferation. Prostate 2002, 52:43–58
38. Steiner GE, Newman ME, Paikl D, Stix U, Memaran-Dagda N, Lee C, Marberger MJ: Expression and function of pro-inflammatory interleukin IL-17 and IL-17 receptor in normal, benign hyperplastic, and malignant prostate. Prostate 2003, 56:171–182
39. Handisurya A, Steiner GE, Stix U, Ecker RC, Pfaffeneder-Mantai S, Langer D, Kramer G, Memaran-Dadgar N, Marberger M: Differential expression of interleukin-15, a pro-inflammatory cytokine and T-cell growth factor, and its receptor in human prostate. Prostate 2001, 49:251–262
40. Sugimoto Y, Koji T, Miyoshi S: Modification of expression of stem cell factor by various cytokines. J Cell Physiol 1999, 181:285–294
41. Imokawa G, Yada Y, Morisaki N, Kimura M: Biological characterization of human fibroblast-derived mitogenic factors for human melanocytes. Biochem J 1998, 330:1235–1239
42. Rodriguez-Nieves JA, Macoska JA: Prostatic fibrosis, lower urinary tract symptoms, and BPH. Nat Rev Urol 2013, 10:546–550
43. Gharaee-Kermani M, Kasina S, Moore BB, Thomas D, Mehra R, Macoska JA: CXC-type chemokines promote myofibroblast phenoconversion and prostatic fibrosis. PLoS One 2012, 7:e49278
44. Ma J, Gharaee-Kermani M, Kunju L, Hollingsworth JM, Adler J, Arruda EM, Macoska JA: Prostatic fibrosis is associated with lower urinary tract symptoms. J Urol 2012, 188:1375–1381